

Cu-Mn: Atomic short-range order, spin-density wave, and spin glass

Y. Tsunoda

Faculty of Science, Osaka University, Toyonaka, Osaka 560 Japan

J. W. Cable

Solid State Division, Oak Ridge National Laboratory, Oak Ridge, Tennessee, 37831

(Received 31 December 1991)

Using a specimen with well-developed atomic short-range order (ASRO), the magnetism of a Cu-Mn alloy was studied by use of a neutron-scattering method. A spin-density wave (SDW) with high Néel temperature ($T_N \sim 400$ K) was observed. The SDW propagates on the ab plane of the well-developed ASRO, which is accompanied by a tetragonal lattice distortion. The type of ASRO, the spin structure of the SDW, and the origin of the spin-glass-like behavior in ordinary Cu-Mn alloys are discussed on the basis of the present experimental data.

I. INTRODUCTION

In the past three decades, many efforts have been devoted to understanding the magnetism of Cu-Mn alloys, which have been regarded as the prototypical spin glass for a long time. The latest important development in this area is the observation by a polarized-neutron technique¹ of magnetic satellite diffuse peaks located at $1\frac{1}{2} \pm \delta 0$ and equivalent symmetry positions at low temperature, together with atomic short-range-order (ASRO) peak at $1\frac{1}{2} 0$. Gotaas, Rhyne, and Werner reported that the satellite-diffuse-peak intensity tends to zero near the spin-glass freezing temperature (T_F) in the elastic limit of the high-resolution neutron-scattering measurement.² From these observations, Werner presented the following understanding on the magnetism of Cu-Mn alloys.³ In contrast with the conventional spin-glass interpretation, the condensation of an incommensurate spin-density wave (SDW) with 12 equivalent Q domains, in concert with the ferromagnetic cluster associated with ASRO, would be the origin of various mysteries of magnetic behavior in this system. Strong inelastic scattering of neutrons centered at the satellite-peak positions and persisting far above T_F seems to support this SDW description of the magnetism of Cu-Mn alloys.⁴ However, several important questions still remain unsolved. For instance, what is the ground state of the magnetism in Cu-Mn alloys, or what is the cause of the difference between the SDW in Cu-Mn and that in other systems?

Cu-Mn alloys always have some degree of ASRO even in drastically quenched specimens. In spite of this fact, atomic long-range order (ALRO) does not become large enough to give an infinitely sharp Bragg peak even after a long period of aging. However, we have now succeeded in growing a single crystal with highly developed ASRO. Since this specimen also has an anisotropic distribution of chemical domains, it provides us with fundamental information on the relation between ASRO and the magnetism of this system. In the present paper, on the basis of neutron-scattering data for this peculiar specimen with

well-developed ASRO, origins of the mysterious magnetic behaviors in Cu-Mn alloys are discussed.

II. SAMPLE PREPARATION AND MEASUREMENT

High-purity Cu (99.999%) and Mn (99.9%) were melted several times in an arc furnace. The single crystal was grown in an alumina crucible using the Bridgman method in an Ar (+H₂ 5%) gas atmosphere. After a homogenization anneal at 750°C for a day, the single crystal was quenched and then aged for the development of the atomic order at 200°C for 2 months.⁵ The nominal Mn concentration of the present specimen was 35 at. %. The actual Mn concentration of the present specimen was determined to be 34.8 at. % by x-ray fluorescence analysis using a piece cut from the same ingot as the present specimen. Neutron-scattering measurements were performed using HB-1A and HB-1 triple-axis spectrometers installed at HFIR, ORNL. A part of the data was taken at the 5-G spectrometer at JRR-3, Tokai.

III. EXPERIMENTAL DATA

A. Elastic neutron scattering

Figure 1 shows the typical experimental line profile observed at room temperature (RT) by an elastic scan along the [010] direction from 100 to 110. On this symmetry line, previous authors observed the diffuse magnetic satellite and ASRO peaks at low temperature and only the latter at RT.^{1,6} However, the present data show a sharp single peak at the satellite-peak position as well as well-developed ASRO peak at $1\frac{1}{2} 0$ even at RT. From the temperature variation of the peak intensity, the sharp peak at $1\frac{1}{2} + \delta 0$ ($\delta \sim 0.18$) is magnetic in origin. The absence of another satellite peak at the symmetry-related position 10.320 is considered to be due to a strong anisotropy of the domain distribution. Then, using this peculiar specimen, we can study the atomic and magnetic symmetries for a single-domain single crystal in more detail.

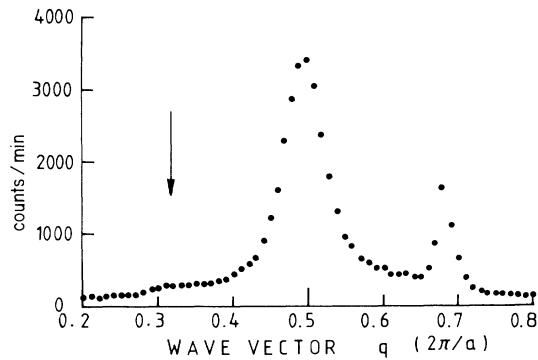


FIG. 1. Typical diffraction pattern observed at RT by scanning along the [010] axis from 100 to 110. Peaks at $q=0.5$ and 0.68 are an atomic order peak and magnetic satellite peak, respectively. An arrow indicates an equivalent magnetic satellite-peak position.

In a cubic crystal, there are 24 lines which are equivalent to the [010] line from 100 to 110 in three-dimensional reciprocal-lattice space. We have studied ASRO and magnetic peaks on all these 24 equivalent [010] lines. In Fig. 2(a) diffraction patterns observed at RT are depicted on the (100) scattering plane, which has

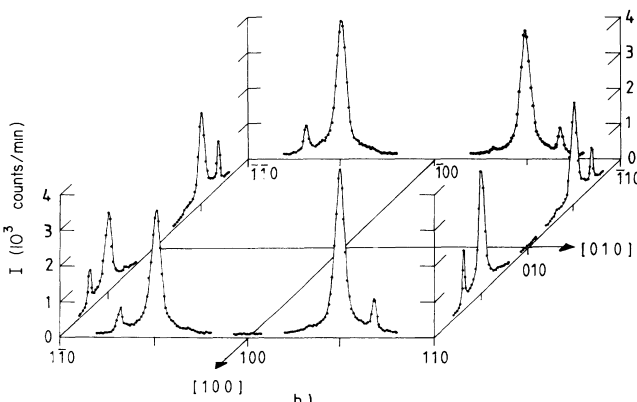
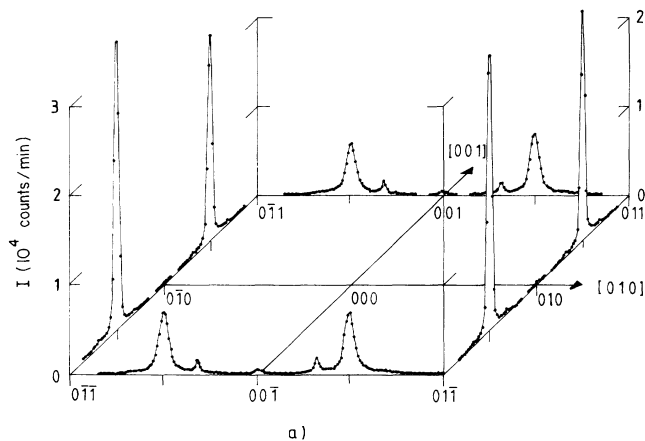


FIG. 2. Diffraction patterns of equivalent-symmetry lines to that of Fig. 1 on (a) the (100) scattering plane and (b) the (001) scattering plane. Note the difference in the scale of the vertical axes.

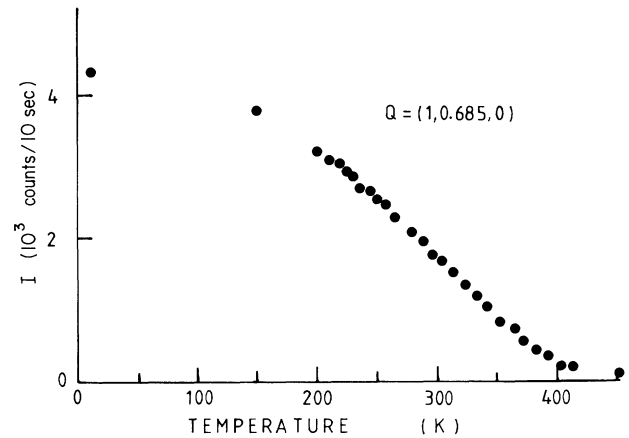


FIG. 3. Temperature dependence of the magnetic satellite-peak intensity.

eight equivalent lines. Diffraction patterns on the (001) scattering plane, which has another eight equivalent lines, are given in Fig. 2(b). The large difference of the intensities of the ASRO peaks at $1\frac{1}{2}0$ and equivalent-symmetry positions on the (100) scattering plane is again ascribed to the anisotropic distribution of domains. [Note that the vertical axes in Figs. 2(a) and 2(b) have different scales.] From the intensity ratio of the ASRO peaks, we can estimate the volume fraction of a predominant domain to be about 70% of the specimen. Thus this specimen is approximately a single-domain single crystal with all of the high-intensity magnetic satellite peaks arising from the predominant domain.

The temperature variation of the magnetic satellite intensity is shown in Fig. 3. The Néel temperature of the SDW is roughly estimated to be 400 K.

B. Tetragonal lattice distortion

Careful examination showed that some magnetic satellite peaks are located slightly inward for the longitudinal

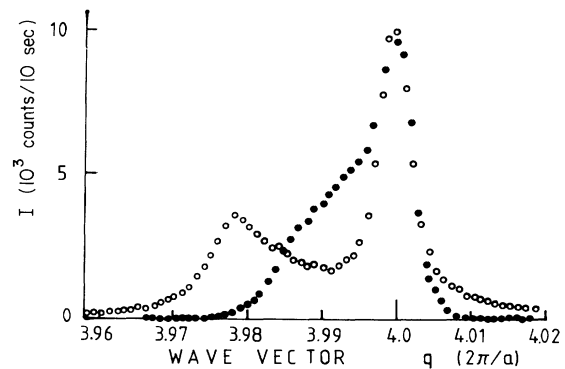


FIG. 4. X-ray-diffraction patterns of longitudinal scan around the 400 Bragg-peak position studied at RT. Open circles are the data for the specimen with well-developed ASRO. Solid circles are for $\text{Cu}_{77}\text{Mn}_{23}$ with ordinary ASRO. Both have extra peaks at the left-hand side of the 400 Bragg peak.

scan, but others are not. In order to check the possibility of tetragonal lattice distortion, an x-ray-diffraction measurement around the 400 Bragg-peak position has been performed. Figure 4 indicates the diffraction pattern observed by scanning along the scattering vector (longitudinal scan). Double peaks are observed in this longitudinal scan, indicating a tetragonal lattice distortion. The fcc lattice expands along the c axis by about 0.5% when atomic order develops. The tetragonal lattice distortion for the specimen with ordinary ASRO has also been studied. The line profile observed around the 400 for a $\text{Cu}_{77}\text{Mn}_{23}$ alloy specimen is also shown in Fig. 4 by the solid circles. Tetragonality is rather small, but lattice distortion still exists even for the ordinary ASRO specimen.

C. Inelastic neutron scattering

In our previous data for the quenched specimen,⁴ the elastic satellite-peak intensity around $1\frac{1}{2} \pm \delta 0$ disappeared almost perfectly at RT, but strong inelastic diffuse scattering at the satellite-peak position was observed far above T_F . However, for the present specimen with well-developed ASRO, the elastic magnetic satellite peak remains even at RT. In order to study the origin of the strong inelasticity at the satellite-peak position, inelastic-scattering measurements were performed for the present specimen with strong anisotropic domain distribution. Several diffraction patterns of constant- E scans along the

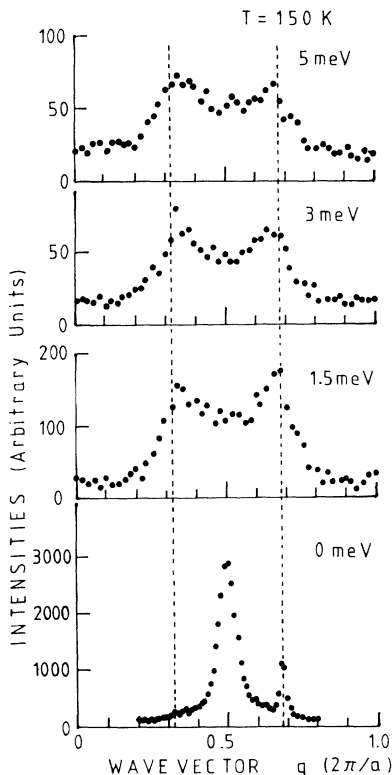


FIG. 5. Elastic and inelastic diffraction patterns observed by scanning along the [010] direction with constant- E mode of operation. Dashed lines indicate the sharp satellite-peak positions for the specimen with well-developed ASRO.

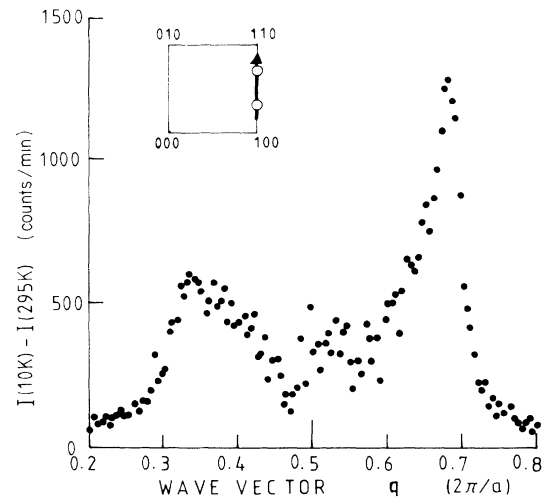


FIG. 6. Elastic magnetic scattering determined by the subtraction of the data at RT from those at 10 K. Each satellite peak is composed of two parts: sharp peaks at $\mathbf{q} = (2\pi/a)(1, 0.32, 0)$ and $\mathbf{q} = (2\pi/a)(1, 0.68, 0)$ and broad peaks, the centers of which are located slightly inside of the sharp peaks.

[010] direction from 100 to 110 are shown in Fig. 5. For the data of the $\Delta E = 0$ scan (elastic scan), the satellite reflection at $\mathbf{q} = (2\pi/a)(1, 0.32, 0)$ is essentially missing because of the anisotropic distribution of domains, but the inelastic scattering appears to be symmetric. Inelastic scattering along the equivalent-symmetry lines on the different scattering planes was also studied, and similar symmetric diffraction patterns with comparable intensities were observed. Furthermore, a careful examination reveals that the maximum peak positions of the inelastic peaks deviate slightly from the sharp satellite-peak positions of the elastic scan. Figure 6 shows an elastic magnetic contribution which is determined by subtraction of the data at RT from those at low temperature (~ 10 K). (This is not the full satellite intensity for the sharp peak at 1,0.68,0 because the T_N of the sharp satellite peak is higher than RT.) There are extra magnetic diffuse peaks, the centers of which are located slightly inside of the sharp satellite peak. These magnetic diffuse peaks are very similar to those observed in the ordinary ASRO specimens. This seems to be the origin of the strong inelastic scattering observed at high temperature. Another point which must be noted in this figure is that there is no well-defined magnetic component at the $1\frac{1}{2}0$ reciprocal-lattice point, although the ASRO peak at that point has a very high intensity.

IV. DISCUSSION

A. ASRO

The ASRO of the Cu-Mn alloy has been investigated by several authors. Sato, Werner, and Yessik⁷ proposed a $D0_{22}$ structure (A_3B composition) for ASRO in a 25 at. % Mn alloy. Hirabayashi *et al.*⁸ claimed a $D1_a$

(Ni₄Mo) type configuration by using their time-of-flight neutron-diffraction data. Bouchiat *et al.*⁹ performed comprehensive x-ray diffraction on ASRO in similar Ag-Mn alloys and discussed the possibility of $I4_1/amd$ (A_2B_2 type) structure and a concentration-wave model. Using the polarized-neutron technique, Cable *et al.*¹ showed that the ASRO parameter observed for 25% Mn alloy was well explained by the A_2B_2 -type structure. All of these structures are members of the $\langle 1\frac{1}{2}0 \rangle$ family, which consists of the stacking of (210)-type planes.

In order to discuss the actual atomic order, the observed high-intensity peaks, which are considered to arise from the predominant domain, are plotted in three-dimensional reciprocal-lattice space in Fig. 7. The high-intensity ASRO peaks are observed at only 8 positions ($\pm 10 \pm \frac{1}{2}$) and ($0 \pm 1 \pm \frac{1}{2}$) of the 24 equivalent peak positions. These are consistent with the superlattice symmetry of the $\langle 1\frac{1}{2}0 \rangle$ family, and the tetragonal axis of the predominant domain (the c axis of the $\langle 1\frac{1}{2}0 \rangle$ family superlattice structure) is parallel to the z axis. However, this still does not determine which structure of the $\langle 1\frac{1}{2}0 \rangle$ family is the most favorable one.

The present experimental data show very few ferromagnetic components around the $1\frac{1}{2}0$ reciprocal-lattice point, although the strong ASRO peak is observed. Instead of that, well-defined magnetic peaks remain at the satellite-peak position even at RT. In contrast with the conclusion reached by previous authors, well-developed ASRO stabilizes the SDW formation, not the ferromagnetic ordering. Then the SDW satellite peaks provide us with some information about ASRO.

Since the sharp magnetic satellite-peak position of the present sample just corresponds to that of the quenched

Cu₇₅Mn₂₅ alloy, the atomically ordered regions of this sample must have a composition near 25% Mn provided that the SDW wavelength does not depend on a degree of the ASRO parameter. The well-known atomically ordered structure of the $\langle 1\frac{1}{2}0 \rangle$ family with this composition is the $D0_{22}$ structure. As was pointed out by previous authors,^{1,8,9} the $D0_{22}$ structure produces superlattice peaks at 001 and 110 with comparable intensity to the $1\frac{1}{2}0$ peak. However, since no such peaks are observed in the present data, a concentration-wave model based on an A_2B_2 structure provides the best description of ASRO in this alloy.

B. Spin-density wave

Since the SDW is stabilized by the atomic order, we have to take the atomic structure into consideration when we discuss the actual magnetic structure of this system. From the distribution of the ASRO-peak intensities, the volume fraction of the predominant domain in this specimen is very high ($\sim 70\%$). Then it is reasonable to assume that all observed high-intensity satellite peaks come from the predominant domain. These are shown in Fig. 7 by the solid circles. The satellite peaks are located only at $(1-\eta)10$ and $(1+\eta)10$ and equivalent positions on the (001) plane. (η is the wave vector measured from 110.) All other satellite peaks reported by previous authors are ascribed to the domain distribution. Note that the SDW propagation vectors exist only on the c plane, suggesting that the c plane has some special character in this type of atomic order. Actually, only on the c plane are the conditions of unlike nearest neighbor and like second neighbor satisfied for the concentration-wave atomic order.

The origin of the SDW modulation is considered to be the Fermi-surface effect, as discussed by previous authors.^{1,3,10-12} This is based on the following experimental facts. (1) Copper has almost a flat Fermi surface along the [110] direction, and the value $2k_F$ for this direction is roughly equal to the distance between the origin and satellite-peak position $11+\eta 0$.¹⁰ (2) the satellite-peak position continuously changes with Mn concentration.^{1,10} (3) Even though the lattice spacing of the Ag-Mn alloy is roughly 10% larger than that in the Cu-Mn alloy, the Ag-Mn alloy also has the same type of magnetic satellite reflection and the satellite-peak positions of both Cu-Mn and Ag-Mn alloys are scaled by the same Mn concentration. This is well understood from the Fermi-surface effect because the Fermi surfaces in these alloys are almost the same in spite of the large difference of Mn-Mn atomic spacing.¹²

The location of the SDW satellite peaks on the c plane determined by the present data is consistent with the previous model of the Fermi-surface effect. Then the fact that the SDW with high Néel temperature is stabilized by well-developed ASRO is understood as follows. Since well-developed ASRO has a good periodicity of atomic configuration, the Fermi surfaces are also well defined and this stabilizes the SDW with high Néel temperature.

One of the remaining mysteries of the SDW in Cu-Mn alloys is an ellipsoidal-shaped diffraction pattern of the

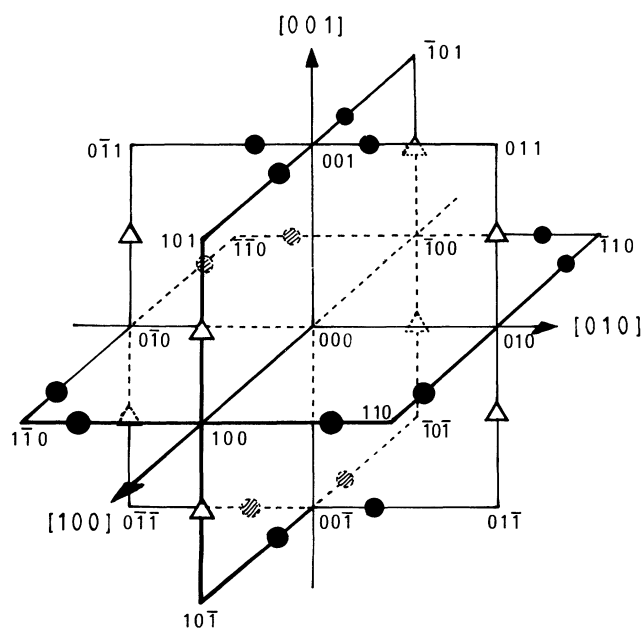


FIG. 7. Observed peak positions in fcc reciprocal-lattice space for the single-domain single crystal. Open triangles indicate atomic order peak positions, and the solid circles are the magnetic satellite-peak positions.

satellite peaks and their directional distribution as given in Fig. 10 of Ref. 1. The tetragonal lattice expansion along the c axis associated with ASRO is so small that the distribution of the tetragonality, which depends on the ASRO cluster size, is not enough to explain this observed ellipsoidal diffraction pattern. It rather seems to be an intrinsic feature of the Cu-Mn SDW; i.e., the correlation length of the SDW on the c plane is longer than that along the c axis. Since the observed tetragonal axis of ASRO is parallel to the ellipticity axis of the satellite peak, the ellipsoidal diffraction pattern of the SDW is a reflection of the actual atomic configuration in ASRO with a tetragonal symmetry. Then, if we take into consideration the location of the satellite peak for the single-domain crystal as shown in Fig. 7 and the equal-domain distribution in an ordinary ASRO specimen, the ellipsoidal shape of the diffraction pattern and directional distribution of the satellites given in Fig. 10 of Ref. 1 are well understood. This is further evidence that the broad SDW satellite peaks for the quenched specimen also arise in the ASRO cluster.

There still exist four propagation directions for the SDW on the c plane of the single- (chemical-) domain single crystal. From neutron-scattering data, it is difficult in principle to distinguish the single-Q SDW state with an equal distribution of magnetic domains from the multiple-Q SDW state. For the present sample, the satellite peaks have nearly the same intensities, as can be seen in Fig. 2. This would be the case for either a multiple-Q SDW state or for a single-Q SDW state with equally populated magnetic domains. However, data for another sample cut from the same ingot show intensities that differ by a factor of 2 for the satellite peaks at the symmetrically equivalent positions $1,0.68,0$ and $0.68,1,0$. This can only result from a single-Q SDW state with unequally populated domains and shows conclusively that the magnetic order of Cu-Mn alloys is a multidomain single-Q SDW state propagating in the c plane along the $[1+\eta 10]$ or $[11+\eta 0]$ directions. (From the viewpoint of the Fermi-surface effect of the SDW, the $[1+\eta 10]$ direction has fundamental meanings rather than the $[1-\eta 10]$ direction.) From the symmetry and intensities of the satellite peaks, we can propose a model of the spin configuration for the Cu-Mn SDW. This spin configuration is shown in Fig. 8 for the b -axis domain. This is basically a type-1 antiferromagnetic structure, but with a helical modulation along the b axis. In this domain the spin at lattice site \mathbf{R} is given by

$$\mathbf{S}(\mathbf{R}) = p(\mathbf{R})S_0[\mathbf{x} \sin(\mathbf{Q}_m \cdot \mathbf{R} + \phi) + \mathbf{z} \cos(\mathbf{Q}_m \cdot \mathbf{R} + \phi)],$$

where $p(\mathbf{R})$ is the number of Mn atoms (0 or 1) at \mathbf{R} , \mathbf{z} is parallel to the tetragonal c axis, ϕ is a phase factor, and \mathbf{Q}_m is the modulation wave vector:

$$\mathbf{Q}_m = 2\pi[\mathbf{a}^* + \mathbf{b}^*(1+\eta)].$$

Such a spin distribution gives satellite peaks at $\mathbf{K} = \tau \pm \mathbf{Q}_m$, where τ is a fundamental reciprocal-lattice vector. Similar expressions for $\mathbf{S}(\mathbf{R})$ and \mathbf{Q}_m are required for the a -axis domain with helical modulation along the a axis.

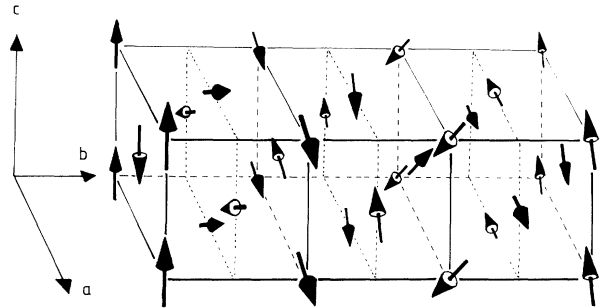


FIG. 8. Spin-structure model of the Cu-Mn SDW. Mn atoms occupy certain positions of fcc cells according to ASRO.

C. Dynamical problem and spin-glass-like behavior

Well-developed ASRO stabilizes the well-defined SDW. Inelastic scattering, however, is not observed at the sharp satellite-peak position. Although the present specimen has strong anisotropy of atomic ordering, the distribution of the inelastic scattering is isotropic and is almost the same as that of the ordinary ASRO specimen. Thus inelastic scattering does not arise from the well-defined SDW stabilized on well-developed ASRO. As pointed out in the experimental data, the present specimen has elastic diffuse satellite peaks slightly inside of the well-defined SDW satellite-peak position. These elastic diffuse peaks are also the same as those observed in the ordinary ASRO specimen. We consider that the present specimen consists of two parts: One part has well-developed ASRO, but the rest of the specimen still has ill-defined ASRO. The broad tails on the ASRO peak at $1 \frac{1}{2} 0$ shown in Fig. 1 support this point. The region with ill-defined ASRO gives strong inelastic scattering around the diffuse satellite-peak position as was observed in the ordinary ASRO specimen. Observation of the magnon excitation from the SDW is usually expected to be very difficult because it has normally an intensity of 10^{-4} of the elastic peak. It is not surprising that there is no inelastic scattering at the well-defined SDW satellite-peak position. It is rather surprising that there is strong inelastic scattering at the diffuse satellite-peak positions.

Unexpectedly strong inelastic diffuse scattering is explained from the viewpoint of the Fermi-surface effect in the SDW. The region with ill-defined ASRO has an ill-defined Fermi surface, resulting in a virtual SDW state with very short lifetime. Werner pointed out³ that this virtual SDW state is very similar to the SDW paramagnon in a paramagnetic $\text{Cr}_{0.95}\text{V}_{0.05}$ alloy recently reported by Fawcett *et al.*¹³ However, there seems to exist an important difference between them. In the latter static SDW formation is suppressed by the introduction of V atoms which change the size and shape of the Fermi surfaces since the alloying effect of the SDW in Cr is explained by a rigid-band model. On the other hand, in the former, the Néel temperature is lowered by the disturbance of the atomic order, i.e., the irregular atomic

configuration which leads to the ill-defined tetragonal lattice distortion and ill-defined Fermi surfaces, resulting in an ill-defined SDW. If the atomic configuration has a good periodicity, the well-defined SDW with high Néel temperature is stabilized, as shown in the present specimen.

The strong inelasticity can also be explained in terms which emphasize the localized spin character. The spin-pair correlation of the SDW inside of the ASRO cluster would be rather strong since the Néel temperature of the SDW in well-developed ASRO is very high. Then each ASRO cluster forms SDW clusters. At RT these clusters behave like the superparamagnetic particles of the SDW. When the temperature is lowered, the frequency of the SDW-cluster fluctuation gradually decreases and finally freezes at T_F because of the coupling between the SDW clusters. On the other hand, the region with well-developed ASRO forms large clusters which are at a standstill even at RT.

The ferromagnetic diffuse scattering around the origin and at $1\frac{1}{2}0$ reported by previous authors can be explained within the SDW-cluster model. In the small ASRO cluster, the SDW-cluster size is also small. The small SDW cluster always has a ferromagnetic component as a result of statistical fluctuations. (For a small magnetic cluster, the number of parallel and antiparallel spins can be expected to differ by the square root of the number of spins.) The dynamical motion and freezing process of these SDW clusters with ferromagnetic components would be the essential ingredient of the spin-glass-like behavior of Cu-Mn alloys.

D. Tetragonal lattice distortion

The tetragonal lattice distortion accompanying with ASRO for Cu-Mn alloys has been observed in the present work. This local lattice distortion is expected to play an important role in determining various properties of this system.

Offering a reason why a Cu-Mn SDW does not extend across the entire crystal, Werner pointed out the topological difficulties due to the existence of 12 equivalent Q domains in the cubic SDW system.³ From the present data, the reason is ascribed to ASRO and the tetragonal lattice distortion accompanying this ASRO. The lattice expansion along the *c* axis supposedly prevents the development of atomic ordering. Then the atomic order remains short ranged. As shown in the present data, the SDW propagates only on the *c* plane of the tetragonal lattice of the ASRO. Thus the SDW never extends across the entire crystal.

The local tetragonal lattice deformation associated

with ASRO also plays the role of an anisotropic energy barrier for the SDW cluster at low temperature. Then a distribution of relaxation times of the SDW clusters results, and spin-glass-like behavior is observed in the ordinary ASRO specimen.

We can speculate that strong anisotropy of the chemical-domain distribution for the present specimen may also be related to the tetragonal lattice distortion. The development of atomic ordering is suppressed under normal conditions because of the lattice deformation energy and would be aided only under special conditions such as under internal strain. Then the appearance probability of the region with well-developed ASRO must be very small, and such a region has a single, tetragonal domain. Thus the specimen with well-developed ASRO often has a strong anisotropic distribution of chemical domains.

In order to estimate the actual Mn concentration of a specimen, it may be possible to use an incommensurability parameter η since satellite-peak position varies with Mn concentration for the ordinary ASRO specimens.^{1,3,10} From the broad satellite-peak position, we can estimate Mn concentration to be about 32 at. % for the present specimen. On the other hand, if we use the data for the sharp satellite peaks of well-developed ASRO, it is estimated to be about 25 at. %. It may seem to be a discrepancy that there are two incommensurability parameters in a specimen. It is plausible that the wavelength of the SDW depends on the degree of the ASRO parameter and ASRO-cluster size because the tetragonality of the lattice deformation associated with ASRO varies with these values in the present specimen.

The present discussion developed here seems to be applicable to rapidly quenched Cu-Mn alloys since the ASRO peak at $1\frac{1}{2}0$ and satellite reflections on both sides of the ASRO peak are always observed by neutron diffraction even for a carefully prepared specimen. A remaining problem is to determine what the low-Mn-concentration limit is for which the present results are applicable.

ACKNOWLEDGMENTS

The authors would like to express their sincere thanks to Dr. N. Wakabayashi for fruitful discussions. A part of the present research was carried out at the Oak Ridge National Laboratory under the U.S.-Japan Cooperation Program in Neutron Scattering and sponsored in part by the U.S. Department of Energy under Contract No. DE-AC05-84OR21400 with Martin Marietta Energy Systems Inc.

¹J. W. Cable, S. A. Werner, G. P. Felcher, and N. Wakabayashi, *Phys. Rev. B* **29**, 1268 (1984).

²J. A. Gotaas, J. J. Rhyne, and S. A. Werner, *J. Appl. Phys.* **57**, 3404 (1985).

³S. A. Werner, *Comments Condens. Matter Phys.* **15**, 55 (1990).

⁴Y. Tsunoda, N. Kunitomi, and J. W. Cable, *J. Appl. Phys.* **57**,

3753 (1985).

⁵The present success in growing highly developed ASRO seems to be rather accidental. Several trials to grow specimens with well-developed ASRO have been made for alloys with different Mn composition, but these have not been successful.

⁶S. A. Werner and J. W. Cable, *J. Appl. Phys.* **52**, 1757 (1981); J.

- W. Cable, A. S. Werner, G. P. Felcher, and N. Wakabayashi, *Phys. Rev. Lett.* **49**, 829 (1982).
- ⁷H. Sato, S. A. Werner, and M. Yessik, in *Magnetism and Magnetic Materials 1971 (Chicago)*, Proceedings of the 17th Annual Conference on Magnetism and Magnetic Materials, edited by D. C. Graham and J. J. Rhyne, AIP Conf. Proc. No. 5 (AIP, New York, 1972), p. 508.
- ⁸M. Hirabayashi, M. Koiwa, S. Yamaguchi, and K. Kamata, *J. Phys. Soc. Jpn.* **45**, 1591 (1978).
- ⁹H. Bouchiat, E. Dartyge, P. Monod, and M. Lambert, *Phys. Rev. B* **23**, 1375 (1981).
- ¹⁰T. M. Harders and P. Wells, *J. Phys. F* **13**, 1017 (1983).
- ¹¹The concept of the SDW in Cu-Mn alloys was proposed by A. W. Overhauser, *J. Phys. Chem. Solids* **13**, 71 (1960).
- ¹²K. Ishibashi, Y. Tsunoda, N. Kunitomi, and J. W. Cable, *Solid State Commun.* **56**, 585 (1985).
- ¹³E. Fawcett, S. A. Werner, A. Goldman, and G. Shirane, *Phys. Rev. Lett.* **61**, 558 (1988).